Supporting Information

to

Easy enrichment of graphitic nitrogen to prepare highly catalytic carbons for oxygen reduction reaction

Javier Quílez-Bermejo[1,*], Sara Pérez-Rodríguez[1], Rafael Canevesi[1], Daniel Torres[1], Emilia Morallón[2], Diego Cazorla-Amorós[3], Alain Celzard[1], Vanessa Fierro[1,*]

[1] Université de Lorraine, Centre National de la Recherche Scientifique (CNRS), Institut Jean Lamour (IJL), F-88000, Épinal, France.

[2] Departamento de Química Física and Instituto de Materiales, Universidad de Alicante, Ap. 99, 03080, Alicante, Spain

[3] Departamento de Química Inorgánica and Instituto de Materiales, Universidad de Alicante, Ap. 99, 03080, Spain.

* Corresponding author.

E-mail address: vanessa.fierro@univ-lorraine.fr (Vanessa Fierro)

Table S1: Bulk, CHN-O contents, measured by elemental analysis, of all carbon materials.

Sample	Carbonization yield / wt. %	C content / wt. %	H content / wt. %	N content / wt. %	O content / wt. %
MSC30	-	*95.15*	*0.55*	*0.30*	*4.00*
MSC30-U1	-	82.46	1.41	7.65	8.48
MSC30-U2	-	78.44	1.62	11.91	8.03
MSC30-U1-700	86	94.94	0.52	3.07	1.47
MSC30-U1-900	82	96.79	0.31	1.83	1.06
MSC30-U1-1100	60	98.67	0.45	0.34	0.55
MSC30-U1-1300	53	98.88	0.33	0.22	0.57
MSC30-U2-700	76	92.02	0.68	5.27	2.03
MSC30-U2-900	64	95.16	0.51	3.06	1.27
MSC30-U2-1100	51	97.62	0.71	0.50	1.17
MSC30-U2-1300	50	99.03	0.27	0.32	0.38

Table S2 : Surface atomic composition, measured by XPS, for pre-treated and heat-treated MSC30 samples, and their relative contents in nitrogen species.

Sample	C / at.%	O / at.%	N / at.%	Graphitic N / at.%	Pyridines / at.%	Pyrroles and pyridones / at.%
MSC30	97.2	2.8	-	-	-	-
MSC30-U1	93.1	2.5	4.4	-	-	-
MSC30-U2	88.8	2.3	8.9	-	-	-
MSC30-U1-700	94.3	3.2	2.5	0.5	1.2	0.8
MSC30-U1-900	96.7	1.7	1.6	0.3	0.8	0.5
MSC30-U1-1100	98.5	1.5	-	-	-	-
MSC30-U1-1300	98.5	1.5	-	-	-	-
MSC30-U2-700	94.3	1.8	4.0	0.4	2.0	1.4
MSC30-U2-900	95.0	2.6	2.6	0.7	1.1	0.9
MSC30-U2-1100	96.9	2.5	0.6	0.6	-	-
MSC30-U2-1300	97.8	2.2	-	-	-	-

Table S3: Electrocatalytic ORR performance of the different materials in this study in an O_2-saturated 0.1 M KOH solution.

Sample	E_{ONSET} / obtained at -0.1 mA·cm^{-2}	$E_{½}$ / V vs RHE	j / mA·cm^{-2} at 0.4 V	n at 0.7 V vs RHE
MSC30	0.82	0.74	-3.7	2.8
MSC30-U1	0.81	0.73	-3.5	3.2
MSC30-U2	0.81	0.73	-3.0	3.2
MSC30-U1-700	0.83	0.72	-4.5	3.4
MSC30-U1-900	0.85	0.74	-5.5	3.6
MSC30-U1-1100	0.85	0.74	-4.9	3.6
MSC30-U1-1300	0.83	0.73	-3.5	3.4
MSC30-U2-700	0.83	0.72	-5.5	3.6
MSC30-U2-900	0.85	0.75	-4.5	3.6
MSC30-U2-1100	0.88	0.78	-5.0	3.8
MSC30-U2-1300	0.86	0.76	-4.3	3.5

Table S4: Electrochemical performance of N-doped carbon materials with the majority of the nitrogen in the form of graphitic or pyridinic N; data obtained from LSV curves at 1600 rpm in an O_2-saturated 0.1 M KOH solution.

Sample	Majority of nitrogen	E_{ONSET} / obtained at -0.1 mA·cm^{-2}	*n* at 0.7 V vs RHE	Reference
MSC30-U2-1100	Graphitic	0.88	3.8	This work
Pt/C	-	0.97	4.0	This work
MW@N1	Pyridines	0.82	3.1	S29
PY-NG	Pyridines	0.70	3.8	S30
NPGN-1:4:10	Pyridines	0.87	3.8	S31
PDA	Pyridines	0.74	3.0	S32
N-FCNFS	Pyridines	0.89	3.9	S33
GC-900	Pyridines	0.88	3.4	S34
PANI-1100	Graphitic	0.93	3.9	S35
NMC	Graphitic	0.91	3.8	S36
NMGC	Graphitic	0.94	3.9	S37
NDCF(H)-H2	Graphitic	0.94	3.9	S38
PDI-900	Graphitic	0.85	4.0	S39
XC72	Non-doped	0.77	2.2	S40
CB	Non-doped	0.79	2.2	S40
CNF	Non-doped	0.81	2.5	S40
SW	Non-doped	0.88	3.8	S40
AC	Non-doped	0.80	2.3	S40
KS4	Non-doped	0.74	2.1	S40
CFAT-C	Non-doped	0.82	3.1	S41
CFAT-B	Non-doped	0.81	2.4	S41
CFAT-A	Non-doped	0.80	2.0	S41

Table S5: Electrochemical performance of the most recently published carbon-based catalysts; data obtained from LSV curves at 1600 rpm in an O_2-saturated 0.1 M KOH solution. N represents nitrogen, Pt represents platinum, S represents sulfur, B represents boron and P represents phosphorus.

Sample	Doping agent(s)	E_{ONSET} / obtained at -0.1 mA·cm^{-2}	Limiting current density / mA·cm^{-2} at 0.4 V	*N* at 0.7 V vs RHE	Reference
MSC30-U2-1100	N	0.88	-5.0	3.8	This work
Pt/C	Pt	0.97	-5.1	4.0	This work
CCA	N	0.90	-4.5	3.7	S1
N-CNF-PHEN-900	N	0.93	-4.9	3.9	S2
NMCS-3	N	0.86	-5.6	3.4	S3
3D-NHPC4	N	0.76	-3.5	3.4	S4
P-PYPZ@700	N	0.86	-4.6	3.8	S5
CPNC-5-950	N	0.91	-4.9	4.0	S6
C-A-N	N	0.93	-5.2	3.7	S7
Z8&NaCl$_{1:1}$-950	N	0.93	-5.5	3.5	S8
PANI-O2-1000-N2-1200	N	0.93	-5.5	4.0	S9
PANI-O2-800	N	0.75	-5.0	3.0	S10
NPCF	N	0.93	-4.7	3.9	S11
NG-C@G-800	N	0.96	-5.6	3.9	S12
BEN-NHCP-1000	N	0.96	-5.4	3.8	S13
ACFP5-800	N	0.85	2.8	2.5	S14
NGO	N	0.75	-2.4	3.2	S15
SN-RGO-900	N, S	0.78	-2	3.8	S16
NB-CDS@CNT	N, B	0.92	-5.8	3.5	S17
XWB-CMP-950	N, S	0.82	-4.7	3.7	S18
NPC	N, P	0.79	-3.2	3.0	S19
PC-N	N, P	0.84	-3.5	3.3	S20
NPLC-3-800	N, P	0.84	-4.1	3.7	S20
NPLC-3-900	N, P	0.68	-1.6	3.0	S21
P-PYPZ@700	N	0.85	-4.6	3.4	S21
JUC-528	N, P	0.82	-3.7	3.8	S22
NS-A-PCM-1000	N, S	0.94	-5.2	3.7	S23
NSP-GRA	N, S, P	0.95	-3.6	3.5	S24
D-NSOCS	N, S	0.92	-6.0	3.9	S25
N-B-C-3H	N, B	0.90	-3.4	4.0	S26
N-PHCNSS-800	N, S	0.92	-5.6	3.8	S27
LC-4	N, S	0.95	-4.0	4.0	S28

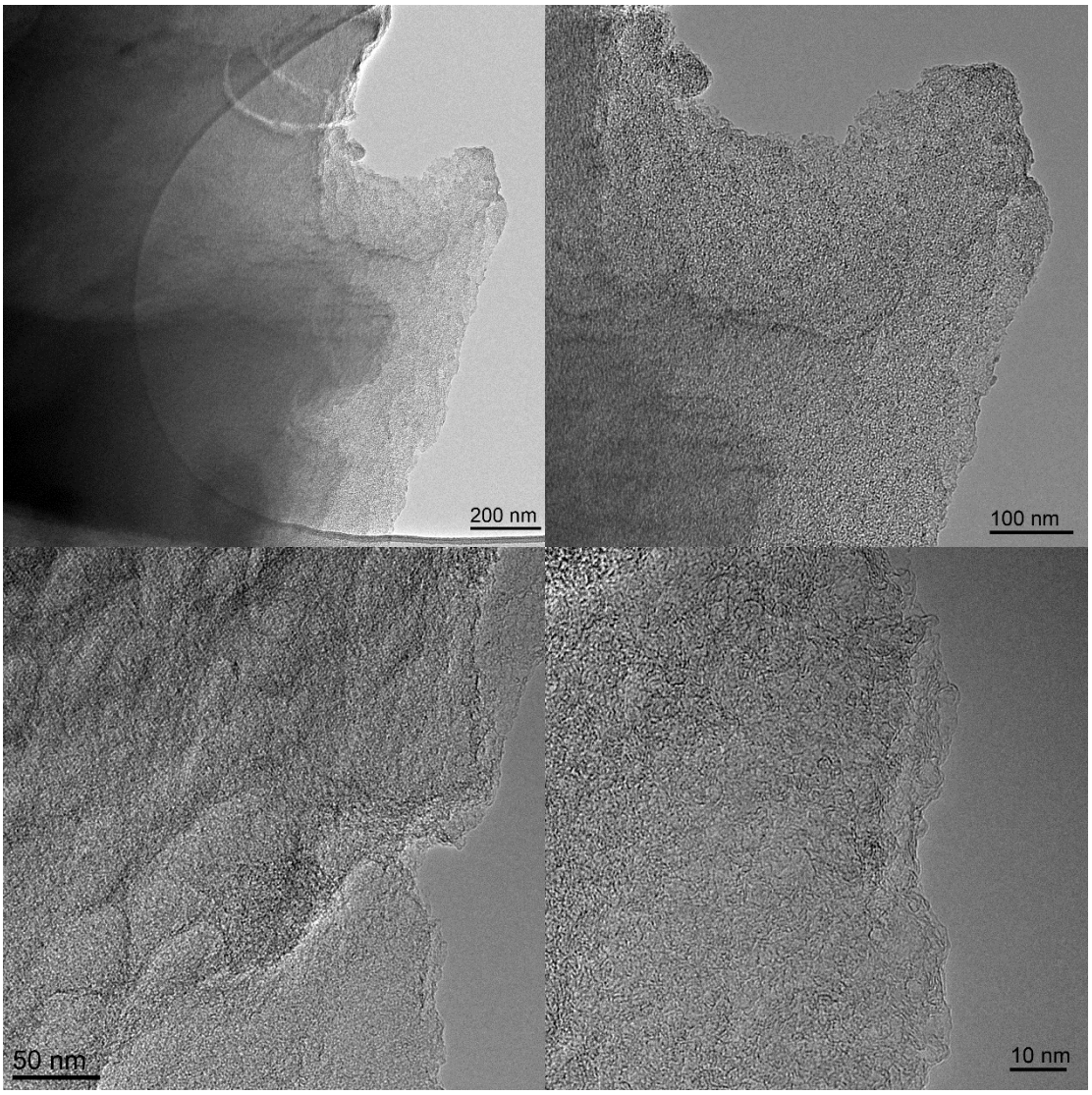

Figure S1: HR-TEM images of MSC30-U1-1100 at different magnifications.

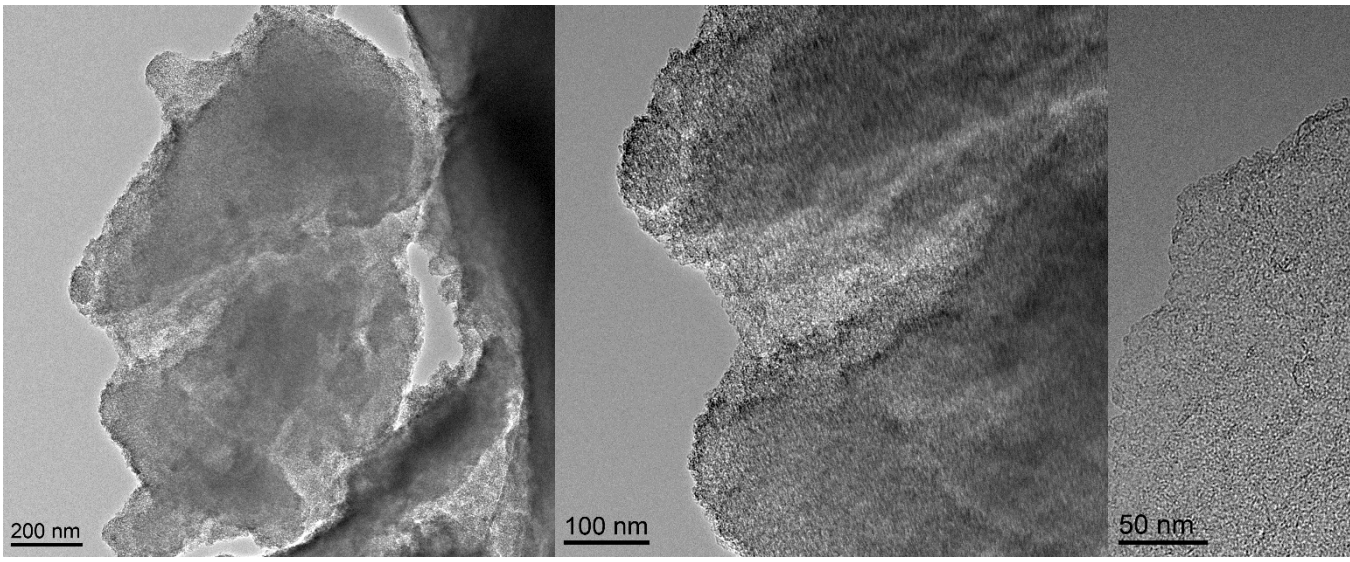

Figure S2: HR-TEM images of MSC30-U2-1100 at different magnifications.

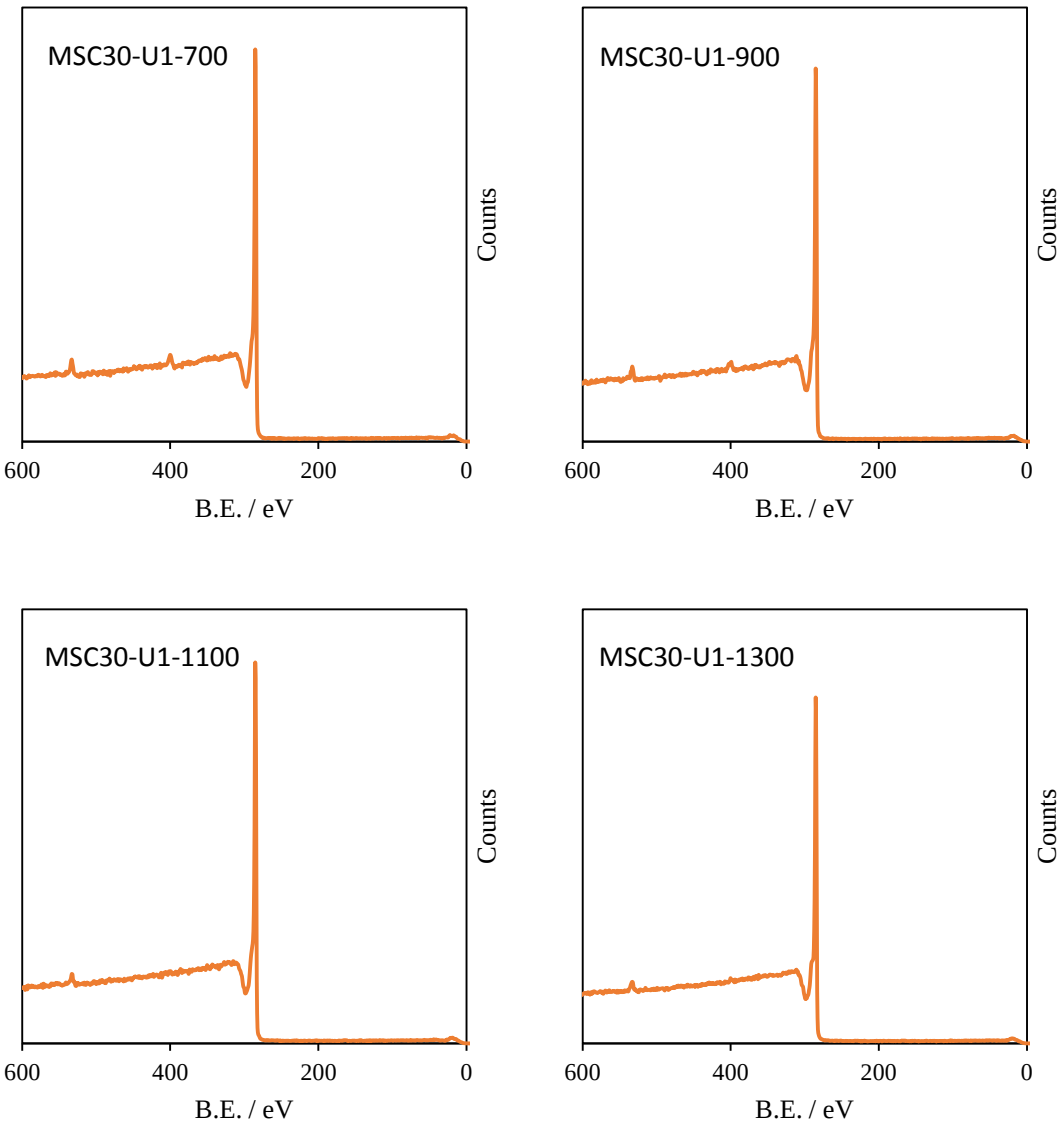

Figure S3: Full XPS spectra of the MSC30-U1-T samples.

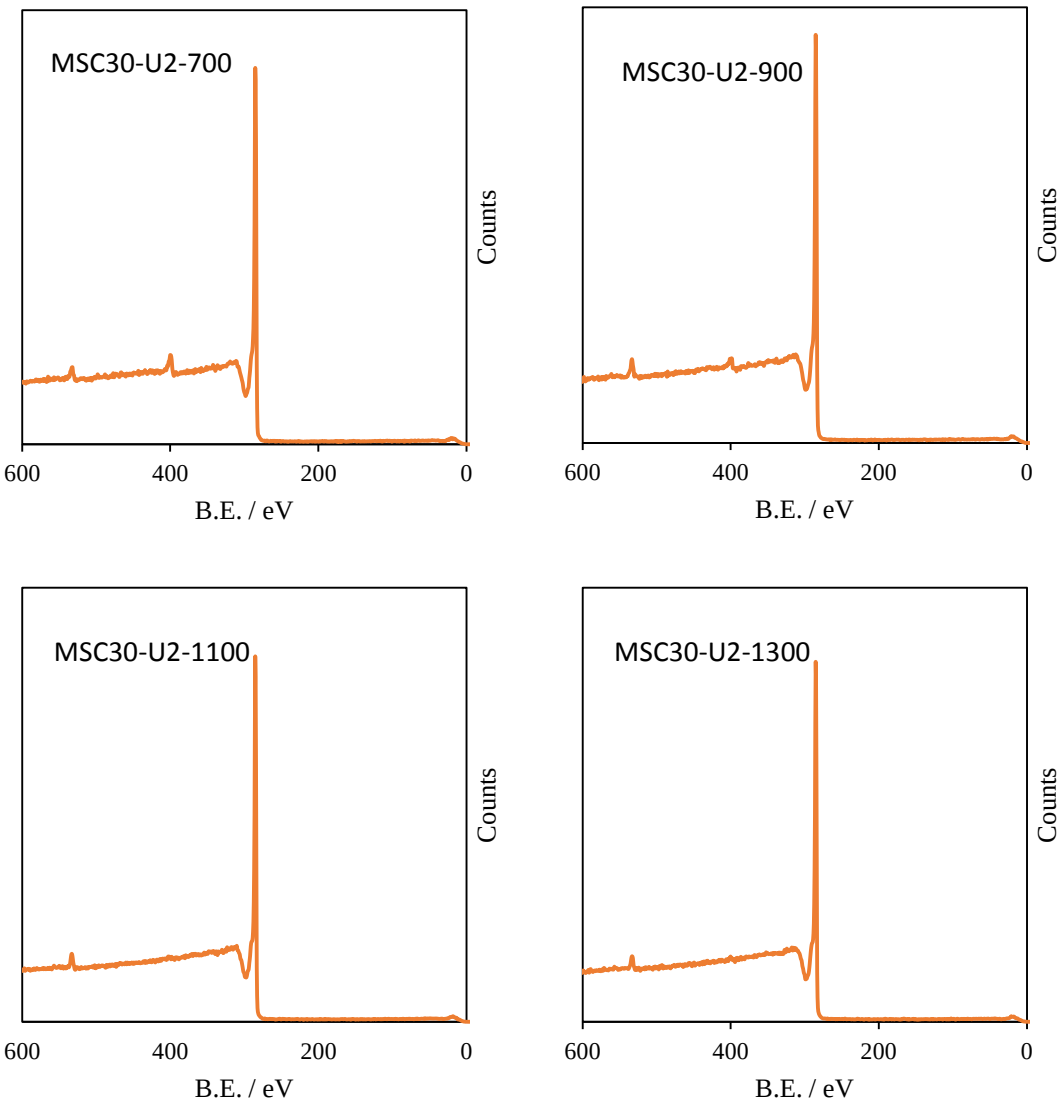

Figure S4: Full XPS spectra of the MSC30-U2-T samples

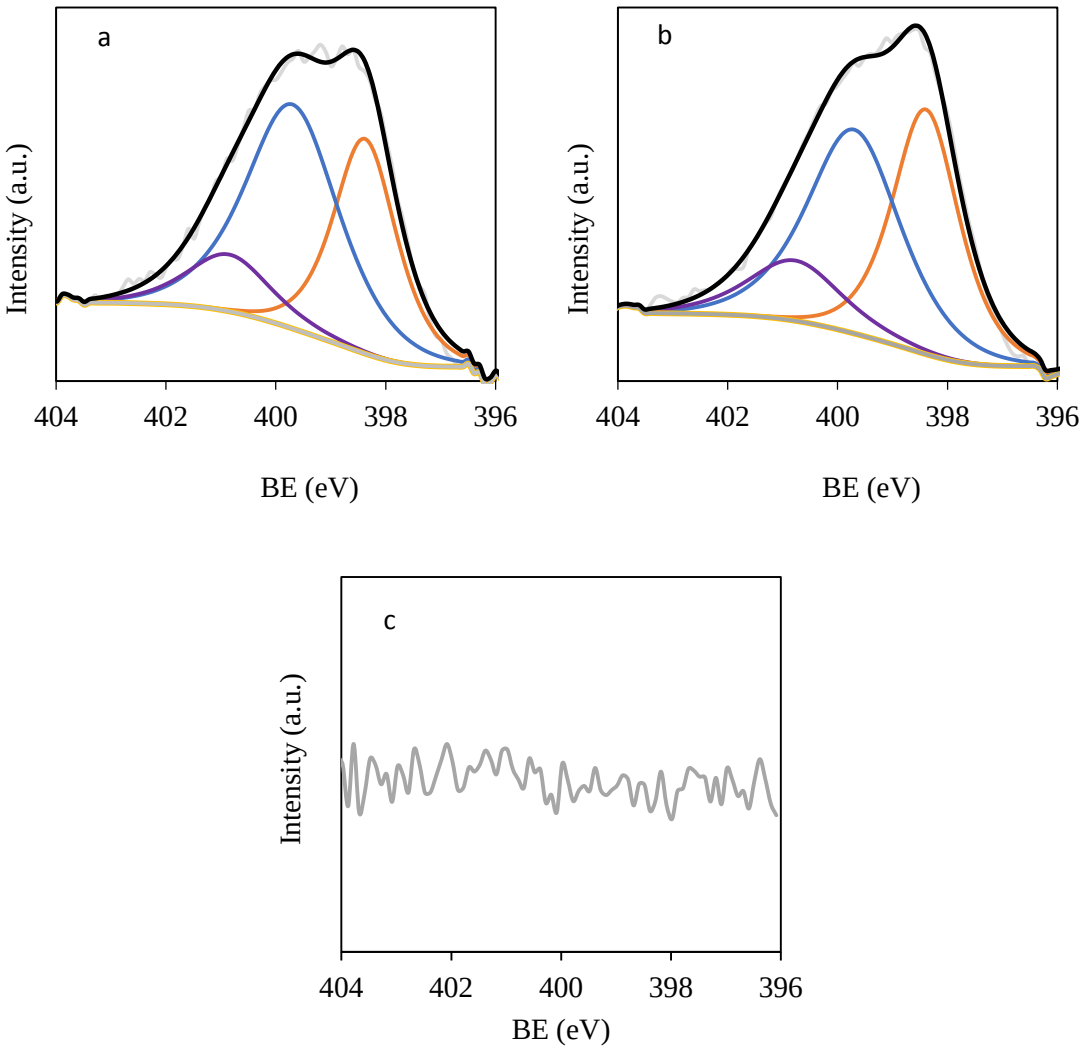

Figure S5: N1s spectra of (a) MSC30-U1, (b) MSC30-U2 and (c) MSC30. Orange peak represents imines, blue peak represents amines and purple peak represents positively charged nitrogen groups.

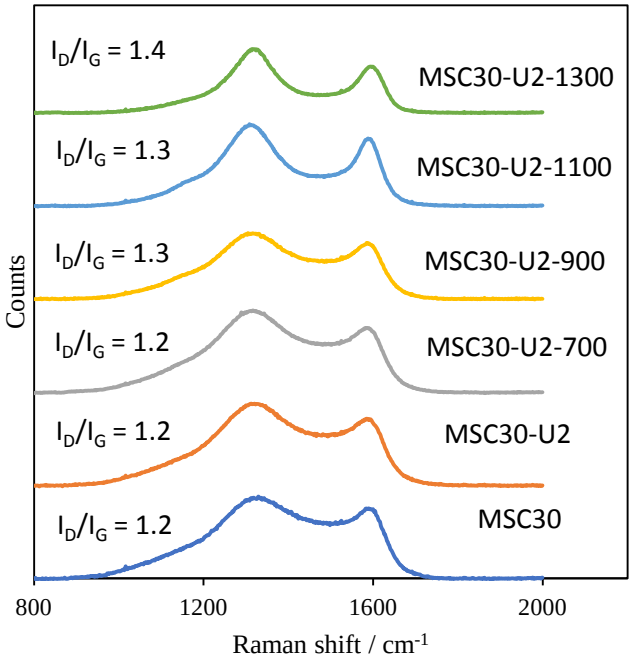

Figure S6: 1st-order Raman spectra of MSC30-U2-T samples obtained at a wavelength of 638 nm.

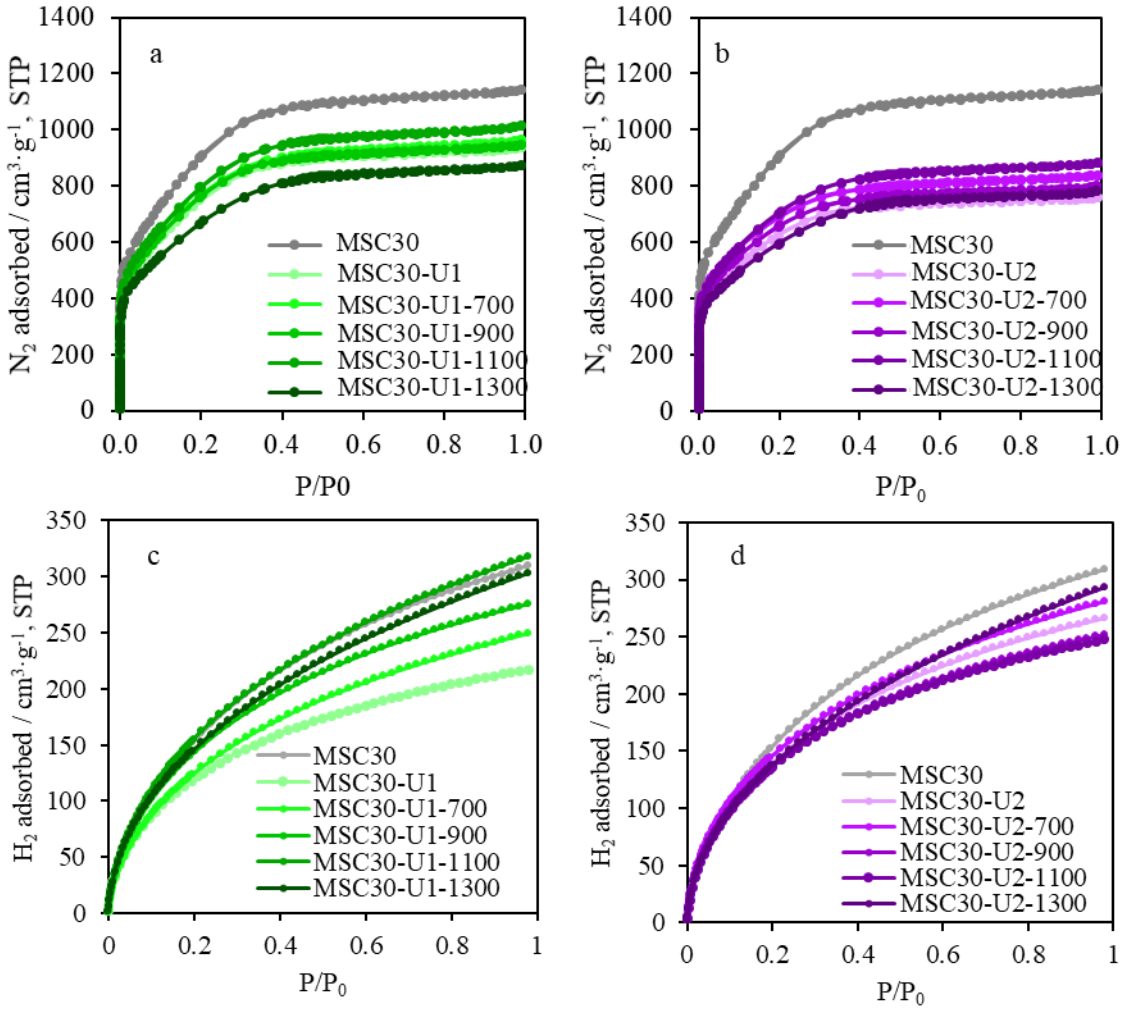

Figure S7: Nitrogen (a,b) and hydrogen (c,d) adsorption isotherms of pristine MSC30 and N-doped carbon materials with the mass ratio carbon to urea of 1:1 (a,c) and 1:2 (b,d).

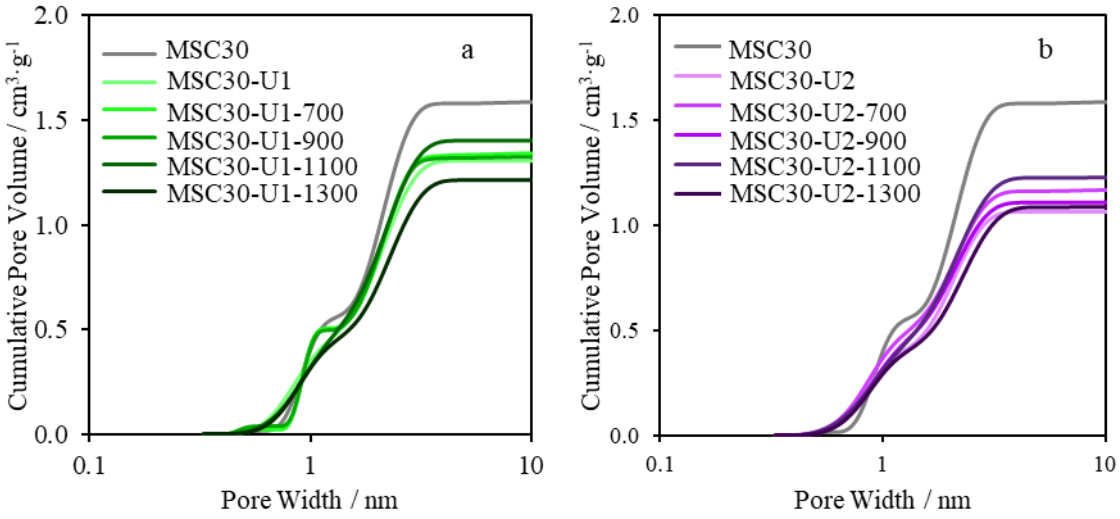

Figure S8: Cumulative pore volumes calculated by 2D-NLDFT model for samples with carbon to urea ratios of 1 (a) and 2 (b).

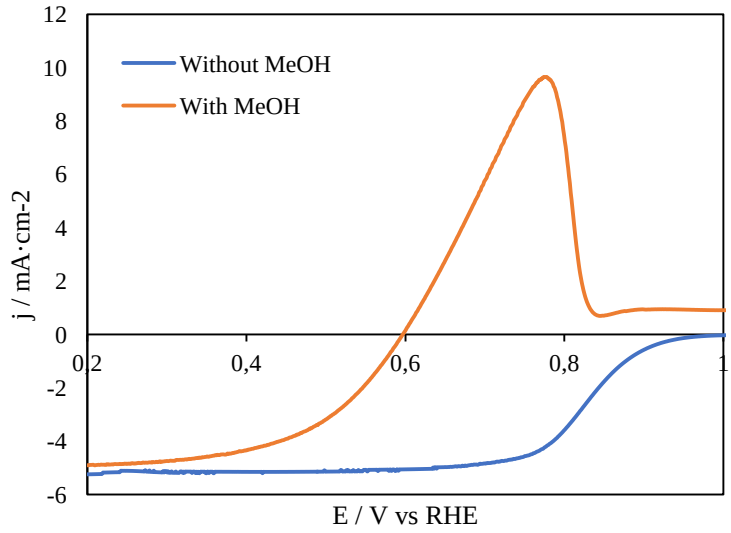

Figure S9: LSV curves of the commercial Pt/C electrocatalyst before and after addition of 1 M methanol in an O_2-saturated 0.1 M KOH solution, at a scan rate of 5 $mV \cdot s^{-1}$.

References

[S1] G. Tuci, C. Zafferoni, A. Rossin, A. Milella, L. Luconi, M. Innocenti, L.T. Phuoc, C. Duong-Viet, C. Pham-huu, G. Giambastiani, Chemically Functionalizated Carbon Nanotubes with Pyridines Groups as Easily Tunable N-decorated Nanomaterials for the Oxygen Reduction Reaction in Alkaline Medium. Chem. Mater. 11 (2014) 3460-3470.

[S2] S. Yasuda, L. Yu, J. Kim, K. Murakoshi, Selective nitrogen doping in graphene for oxygen reduction reactions. Chem. Comm. 49 (2013) 9627-9629.

[S3] Y. Liu, B. He, C. Qi, Nitrogen-Doped Porous Graphene-like Carbon Nanosheets as Efficient Oxygen Reduction Reaction Catalysts under Alkaline and Acidic Conditions. Ind. Eng. Chem. Res. 1 (2021) 210-217.

[S4] O.L. Li, S. Chiba, Y. Wada, G. Panomsuwan, T. Ishizaki, Synthesis of graphitic-N and amino-N in nitrogen-doped carbon via a solution plasma process and exploration of their synergic effect for advanced oxygen reduction reaction. J. Mater. Chem. A 5 (2017) 2073-2082.

[S5] M. Sun, X. Wu, X. Deng, W. Zhang, Z. Xie, Q. Huang, B. Huang, Synthesis of pyridinic-N doped carbon nanofibers and its electro-catalytic activity for oxygen reduction reaction. Mater. Lett. 220 (2018) 313-316.

[S6] C. Maouche, Y. Zhou, B. Li, C. Cheng, Y. Wu, J. Li, S. Gao, J. Yang, Thermal treated three-dimensional N-doped graphene as efficient metal free-catalyst for oxygen reduction reaction. J. Electroanal. Chem. 853 (2019) 113536.

[S7] J. Quílez-Bermejo, E. Morallón, D. Cazorla-Amorós, Oxygen-reduction catalysis of N-doped carbons prepared via heat treatment of polyaniline at over 1100ºC. Chem. Comm. 54 (2018) 4441-4444.

[S8] J. Quílez-Bermejo, K. Strutnski, M. Melle-Franco, E. Morallón, D. Cazorla-Amorós, On the Origin of the Effect of pH in Oxygen Reduction Reaction for Nondoped and Edge-type Quaternary N-Doped Metal-Free Carbon-Based Catalysts. ACS Appl. Mater. Interfaces 12 (2020) 54815-54823.

[S9] X. Wu, K. Chen, Z. Lin, Y. Zhang, H. Meng, Nitrogen doped graphitic carbon from biomass as non noble metal catalysts for oxygen reduction reaction. Mater. Today 13 (2019) 100-108.

[S10] J. Luo, K. Wang, X. Hua, W. Wang, J. Li, S. Zhang, S. Chen, Pyridinic-N Protected Synthesis of 3D Nitrogen-Doped Porous Carbon with Increased Mesoporous Defects for Oxygen Reduction. Small 15 (2019) 1805325.

[S11] R. Liu, D. Wu, X. Feng, K. Müllen, Nitrogen-Doped Ordered Mesoporous Graphitic Arrays with High Electrocatalytic Activity for Oxygen Reduction. Angewandte Chem. Int. 49 (2010) 2565-2569.

[S12] A. Gabe, R. Ruiz-Rosas, E. Morallón, D. Cazorla-Amorós, Understanding of oxygen reduction reaction by examining carbon-oxygen gasification reaction and carbon active sites on metal and heteroatoms free carbon materials of different porosities and structures. Carbon 148 (2019) 430-440.

[S13] M. Seredych, A. Szczurek, V. Fierro, A. Celzard, T. Bandosz, Electrochemical Reduction of Oxygen on Hydrophobic Ultramicroporous PolyHIPE Carbon. ACS Catal. 8 (2016) 5618-5628.

[S14] J.C. Carrillo-Rodríguez, A.M. Garay-Tapia, B. Escobar-Morales, J. Escorcia-Garcia, M.T. Ochoa-Lara, F.J. Rodríguez-Varela, I.L. Alonso-Lemus; Insight into the performance and stability of N-

doped Ordered Mesoporous Carbon Hollow Spheres for the ORR: Influence of the nitrogen species on their catalytic activity after ADT. Int. J. Hydrog. Energy 2021, 46, 26087-26100.

[S15] G.A. Ferrero, A.B. Fuertes, M. Sevilla, M.M. Titirici, Efficient metal-free N-doped mesoporous carbon catalysts for ORR by a template-free approach. Carbon 2016, 106, 179-187.

[S16] J. Zhang, M. Lv, D. Lui, L. Du, Z. Liang, Nitrogen-doped carbon nanoflower with superior ORR performance in both alkaline and acidic electrolyte and enhanced durability. Int. J. Hydrog, Energy 2018, 43, 4311-4320.

[S17] J. Tang, J. Liu, C. Li, Y. Li, M.O. Tade, S. Dai, Y. Yamauchi. Synthesis of nitrogen-doped mesoporous carbon spheres with extra-large pores through assembly of deblock copolymer micelles. Angew. Int. Ed. 2014, 54, 588-593.

[S18] J. Liu, X. Shan, G. Wang, W. Kong. Meso-macroporous Carbons Decorated with Ample Nitrogen Sites as Bifunctional Catalysts in CO2 Catalytic Conversoin and Oxygen Reduction Reaction. ChemistrySelect 2021, 6, 1570-1578.

[S19] R. Cao, F. Hu, T. Zhang, W. Shao, S. Liu, X. Jian, Bottom-up fabrication of triazine-based frameworks as metal-free materialsfor supercapacitors and oxygen reduction reaction. RSC Adv. 2021, 11, 8384-8393.

[S20] J. Qi, B. Jin, W. Liu, W. Zhang, L. Xu. Converting coals into carbon-based pH-universal oxygen reduction catalysts for fuel cells. Fuel 2021, 285, 119163.

[S21] P. Chen, J. Zang, S. Zhou, S. Jia, P. Tian, H. Cai, H. Gao, Y. Wang. N-doped 3D porous carbon catalyst derived from biowaste Triarrhena saccharifloraa panicle for oxygen reduction reaction. Carbon 2019, 146, 70-77.

[S22] Y. Cao, Z. Liu, Y. Tang, Z. Wang, F. Liu, Y. Wen, B. Shan, R. Chen. Vaporized-salt-induced sp3 - hybridized defects on nitrogen-doped carbon surface towards oxygen reduction reaction. Carbon 2021, 180, 1-9.

[S23] J. Quílez-Bermejo, M. Melle-Franco, E. San-Fabián, E. Morallón, D. Cazorla-Amorós, D. Towards Understanding the Active´ Sites for the ORR in N-Doped Carbon Materials through FineTuning of Nitrogen Functionalities: An Experimental and Computational Approach. J. Mater. Chem. A 7 (2019) 24239−24250.

[S24] J. Quílez-Bermejo, C. Gonzalez-Gaitán, E. Morallón, D. Cazorla-Amorós, Effect of Carbonization Conditions of Polyaniline on Its´ Catalytic Activity towards ORR. Some Insights about the Nature of the Active Sites. Carbon 119 (2017) 62−71.

[S25] J. Min, X. Xu, J. Koh, J. Gong, X. Chen, J. Azadmanjiri, F. Zhang X. Wen, C. He, Brachned Poly(L-lysine)-Derived Nitrogen-Containing Porous Carbon Flake as the Metal-Free Electrocatalyst towards Efficient Oxygen Reduction Reaction. ACS Appl. Energy Mater. 4 (2021) 3317-3326.

[S26] H. Begum, M.S. Ahmed, Y-B. Kim, Nitrogen-rich graphitic-carbon@graphene as a metal-free electrocatalyst for oxygen reduction reaction. Scient. Reports, 10 (2020) 12431.

[S27] Y. Yang, Z. He, S. Wang, H. Wang, G. Zhu, Hyper-Crosslinked Polymer-Derived Nitrogen-Doped Hierarchical Porous Carbon as Metal-Free Electrocatalysts for High-Efficiency Oxygen Reduction. Energy Fuels 23 (2021) 19614-19623.

[S28] A.C. Ramírez-Pérez, J. Quílez-Bermejo, J.M. Sieben, E. Morallón, D. Cazorla-Amorós, Effect of Nitrogen-Functional Groups on the ORR Activity of Activated Carbon Fiber-Polypyrrole-Based Electrodes. Electrocatalysis 9 (2018) 697-705.

[S29] G. Periyasamy, K. Annamalai, I.M. Patil, B. Kakade, Sulfur and nitrogen co-doped rGO sheets as efficient electrocatalyst for oxygen reduction reaction in alkaline medium. Diam. Relat. Mater. 114 (2021) 108338.

[S30] Y. Pei, H. Song, Y. Liu, Y. Cheng, W. Li, Y. Chen, Y. Fan, B. Liu, S. Lu, Boron-nitrogen-doped carbon dots on multi-walled carbon nanotubes for efficient electrocatalysis of oxygen reduction reactions. J. Colloid Interface Sci. 600 (2021) 865-871.

[S31] S-B. Ren, X-L. Chen, P-X. Li, D-Y. Hu, H-L. Liu, W. Chen W-B. Xie, Y. Chen, X-L. Yang, D-M. Han, G-H. Ning, X-H. Xia. Nitrogen and sulfur dual-doped carbon nanotube derived from a thiazolothiazole based conjugated microporous polimer as efficient metal-free electrocatalysts for oxygen reduction reaction. J. Power Sources 461 (2020) 228145.

[S32] H-J. Zhang, J. Geng, C. Cai, Z-F. Ma, Z. Ma, W. Yao, J. Yang, Effect of doping order on metal-free heteroatoms dual-doped carbon as oxygen reduction electrocatalyst. Chin. Chem. Lett. 32 (2021) 745-749.

[S33] B. Zheng, J. Wang, Z. Pan, X. Wang, S. Liu, S. Ding, L. Lang, An efficient metal-free catalyst derived from waste lotus seedpod for oxygen reduction reaction. J. Porous Mater. 27 (2020) 637-646.

[S34] R. Cao, F. Hu, T. Zhang, W. Shao, S. Liu, X. Jian, Botton-up fabrication of triazine-based frameworks as metal-free materials for supercapacitors and oxygen reduction reaction. RSC Adv. 11 (2021) 8384-8393.

[S35] D. Li, C. Li, L. Zhang, H. Li, L. Zhu, D. Yang, Q. Fang, S. Qiu, X. Yao. Metal-Free Thiophene-Sulfur Covalent Organic Framework: Precise and Controllable Synthesis of Catalytic Active Sites for Oxygen Reduction. J. Am. Chem. Soc. 142 (2020) 8104-8108.

[S36] H. Lu, C. Yang, J. Chen, J. Li, H. Jin, J. Wang, S. Wang. Tailoring Hierarchically Porous Nitrogen-, Sulfur-Codoped Carbon for High-Performance Supercapacitors and Oxygen Reduction. Small 16 (2020) 1906584.

[S37] Y. Wang, N. Xu, R. He, L. Peng, D. Cai, J. Qiao, Large-scale defect-engineering tailored tri-doped graphene as a metal-free bifunctional catalyst for superior electrocatalytic oxygen reaction in rechargeable Zn-air battery. Appl. Catal. B 285 (2021) 119811.

[S38] S. Zhou, J. Zang, H. Gao, X. Tian, P. Tian, S. Song, Y. Wang, Deflagration method synthesizing N, S co-doped oxygen-functionalized carbons as a bifunctional catalyst for oxygen reduction and oxygen evolution reaction. Carbon 181 (2021) 234-245.

[S39] W. Wang, P. Wang, Y. Kang, J. Zhao, P. Tao, Z. Lei, Flame synthesis of nitrogen, boron co-doped carbon as efficient electrocatalyst for oxygen reduction reaction. Int. J. Hydrog. 44 (2019) 4771-4779.

[S40] Z. He, P. Wai, T. Xu, J. Han, X. Gao, X. Liu, Defect-rich N/S-co-doped porous hollow carbon nanospheres derived from fullerenes as efficient electrocatalysts for the oxygen-reduction reaction and Zn-air batteries. Mater. Chem. Front. 5 (2021) 7873-7882.

[S41] Y. Shen, F. Peng, Y. Cao, J. Zuo, H. Wang, H. Yu, Preparation of nitrogen and sulfur co-doped ultrathin graphitic carbon via annealing bagasse lignin as potential electrocatalyst towards oxygen reduction reaction in alkaline and acid media. J. Energy Chem. 34 (2019) 33-42.